Journal Pre-proofs

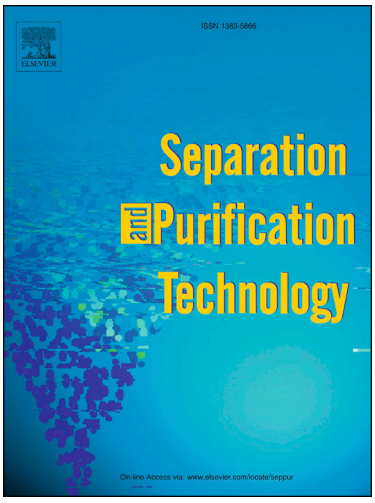

Separation of mandelic acid enantiomers using solid-liquid biphasic systems with chiral ionic liquids

Mariam Kholany, Francisca A. e Silva, Tânia E. Sintra, Paula Brandão, Sónia P.M. Ventura, João A.P. Coutinho

PII: S1383-5866(20)31942-0
DOI: https://doi.org/10.1016/j.seppur.2020.117468
Reference: SEPPUR 117468

To appear in: *Separation and Purification Technology*

Received Date: 31 March 2020
Revised Date: 16 July 2020
Accepted Date: 22 July 2020

Please cite this article as: M. Kholany, F.A. e Silva, T.E. Sintra, P. Brandão, S.P.M. Ventura, J.A.P. Coutinho, Separation of mandelic acid enantiomers using solid-liquid biphasic systems with chiral ionic liquids, *Separation and Purification Technology* (2020), doi: https://doi.org/10.1016/j.seppur.2020.117468

Separation of mandelic acid enantiomers using solid-liquid biphasic systems with chiral ionic liquids

Mariam Kholany[1], Francisca A. e Silva[1], Tânia E. Sintra[1], Paula Brandão[1], Sónia P. M. Ventura[1], João A. P. Coutinho[1]*

[1]CICECO - Aveiro Institute of Materials, Department of Chemistry, University of Aveiro, 3810-193 Aveiro, Portugal

*Corresponding author – E-mail address: jcoutinho@ua.pt (J. A. P. Coutinho)

Abstract

This work aims to take full advantage of ionic liquids' (ILs) "designer solvent" nature in order to expand the applicability of solid-liquid biphasic systems (SLBS) as alternative chiral resolution techniques. To this purpose, twelve chiral ILs, bearing chirality on the cation or the anion, were used as chiral selectors in SLBS to selectively precipitate mandelic acid enantiomers. The precipitation studies were performed using aqueous solutions of the chiral ILs or their chiral precursors, where the impact of the chemical structure and chirality was investigated. The most efficient chiral ILs were employed to evaluate the influence of different operational conditions on the formed precipitate, namely resolution time, resolution speed, temperature, initial concentration of chiral IL, initial concentration of racemic mandelic acid and water content. When compared to their precursors, chiral ILs showed an enhanced ability to induce enantioselective precipitation. The composition of the precipitate formed, and the molecular-level mechanisms leading to enantioselective precipitation, were also uncovered. Due to cooperative interactions between the chiral IL and the target mandelic acid enantiomer, the $[N_{4444}]$[D-Phe]-based SLBS proposed allowed to obtain maximum enantiomeric excess of 51% in a single-step, without any further additives.

Keywords: Solid-liquid biphasic systems, Chiral ionic liquids, Enantioseparation, Mandelic acid, Enantiomeric excess

Introduction

The optical isomers of a molecule can be differentiated by the human body, notwithstanding their very similar physical and chemical properties (apart from their optical rotation).[1] Most often, only one of the enantiomers (the eutomer) exerts the desired pharmacological activity, whilst the other (the distomer) might be inert, nefarious or even responsible for unpredictable and undesired side effects.[2,3] Although the commercialization and consumption of some racemic drugs may be safe, the responsible regulatory entities are strict and oblige pharma companies to provide detailed pharmacologic, pharmacokinetic and toxicological data for each enantiomer and the corresponding racemate.[4] Aiming to foster the production of safer and more effective drugs, there is a growing demand for enantiopure compounds instead of their racemic counterparts.

The production of enantiopure drugs has endured numerous challenges.[5] Even though the direct synthesis of the enantiomer carried through asymmetric synthesis is admittedly effective, it is often achieved with cumbersome processes, expensive enantiopure raw materials or catalysts, and must face short development times due to strict time-to-market impositions.[6] Racemic synthesis followed by enantioseparation appears as a propitious alternative to be pursued due to operational simplicity, reduced time-to-market as well as remarkable performance and cost-effectiveness.[7] Several chiral resolution methods have been explored to achieve this goal.[7,8] While chromatography and crystallization represent the most commonly adopted techniques, other alternative approaches, such as kinetic resolution, membrane separation and enantioselective liquid-liquid extraction are gaining momentum.[8–10]

Ionic liquids (ILs) comprise a class of alternative solvents with remarkable structural diversity due to the variety of cations and anions to be used in their synthesis, being these recognized as “designer solvents”.[11,12] By the careful design of ILs using cations and/or anions bearing chirality, the opportunity to create chiral ILs stands out. The first-ever reported chiral IL was 1-butyl-3-methylimidazolium lactate[13] and, since then, the number of available chiral ILs rapidly increased. Chiral ILs can be synthesized from carbohydrates,[14,15] amino acids[16,17] and other natural organic acids,[18] alkaloids[19] and terpenes.[20] Due to the ready availability of most of these natural chiral starting materials, chiral ILs have been used in a myriad of chiral applications,[21] particularly in enantioseparation processes. The use of chiral ILs as ligands or mobile

phase additives in chromatographic and electrophoretic techniques has posed significant progress in the field.[22] Also, more cost-effective and scalable enantioseparation techniques have been reported by exploring the chiral ILs dual function as chiral solvent/chiral selector to develop conventional enantioselective liquid-liquid extractions,[23,24] enantioselective liquid-liquid extractions based on aqueous biphasic systems[25–28] or three-phase partitioning.[28] So far, however, these strategies failed to afford complete enantioseparations[24,25,27] or relied on the use of additives to improve their efficiency.[23,26,28]

Considering the useful role of ILs in the precipitation or crystallization of several compounds,[29,30] including drugs,[31,32] solid-liquid biphasic systems (SLBS) composed of aqueous solutions of chiral ILs emerged as promising tools for enantioseparations.[33–36] This technique affords the enantioselective precipitation of only one enantiomer in a racemic mixture in a simpler and quicker way than enantioselective liquid-liquid extractions, aqueous biphasic systems and three-phase partitioning. Some chiral ILs, namely imidazolium-, pyrrolidinium-, tropine- and ammonium-based bearing L-proline as the anion moiety, were used in SLBS to carry the enantiomeric separation of racemic amino acids [e.g., L-phenylalanine (L-Phe)].[33–35] Such systems combined aqueous solutions of chiral ILs with copper salts as coordination agents to promote enantioselective precipitation, allowing the simultaneous separation and recovery of the target enantiomer. After optimizing SLBS conditions, maximum enantiomeric excesses of 99% of L-Phe in the solid-phase and 67% of D-Phe in the liquid-phase were attained. As further unveiled by spectroscopic techniques and molecular dynamic simulations, it was possible to attribute the enantioselective precipitation to the stronger cooperative interactions of the L-Phe with the chiral IL and the copper ion.[33–35] The industrial interest of chiral IL-based SLBS was further reinforced by performing scale-up studies, attesting recycling and reuse of the chiral IL, cooper salt and Phe enantiomers remaining in solution and covering other amino acids.[34,35] Recently, Cai et al.[36] synthesized four novel chiral ILs incorporating a chiral ureido group to perform the enantiomeric separation and recognition of mandelic acid and its derivatives. By NMR spectroscopy and DFT calculations, the authors attested the pivotal role of strong hydrogen bonding to induce enantioselective precipitation of mandelic acid enantiomers.[36] Up to date, and although chiral IL-based SLBS have shown great promise, the chiral ILs structures investigated remain limited and target racemic compounds covered are mostly confined to amino acids.[33–35]

This work aims to boost the applicability of chiral IL-based SLBS by exploring the chiral ILs structural versatility and expanding the type of racemic mixtures covered. To this purpose, twelve chiral ILs bearing either chiral cations or chiral anions, based on amino acids, amino alcohols and alkaloids, were synthesized and used to develop new SLBS. The ability of these chiral ILs to induce the enantioselective precipitation was evaluated and further optimized using mandelic acid, a poorly studied chiral compound in the context of SLBS.[36] For comparison, the capacity of chiral ILs to cause enantioselective precipitation was evaluated against the corresponding chiral precursors. Additionally, the composition of the solid-phase as well as the interactions occurring between mandelic acid enantiomers and chiral ILs enabling enantioselective precipitation are here addressed.

Experimental section

Chemicals/Materials

Two series of chiral ILs, namely those bearing chiral anions or chiral cations, were investigated. The chiral ILs with chiral anions synthesized in this work were: tetrabutylammonium L-phenylalaninate, $[N_{4444}]$[L-Phe]; tetrabutylammonium D-phenylalaninate, $[N_{4444}]$[D-Phe]; (2-hydroxyethyl)trimethylammonium L-phenylalaninate, [Ch][L-Phe]; (2-hydroxyethyl)trimethylammonium D-phenylalaninate, [Ch][D-Phe]; (2-hydroxyethyl)trimethylammonium L-alaninate, [Ch][L-Ala]; and di(tetrabutylammonium) L-glutamate, $[N_{4444}]_2$[L-Glu]. For the synthesis of these chiral ILs, the reagents used were the tetrabutylammonium hydroxide, $[N_{4444}]$[OH] (40 wt% in water); cholinium hydroxide, [Ch][OH] (45 wt% in methanol); L-phenylalanine, L-Phe (purity = 99.0 wt%); and D-phenylalanine, D-Phe (purity > 98 wt%) acquired from Sigma-Aldrich; L-glutamic acid, L-Glu (purity = 99 wt%) purchased from Riedel-de-Haën; and L-alanine, L-Ala (purity = 99 wt%) acquired from Acros Organics. The chiral ILs with chiral cations synthesized in this work were the 1-methyl quininium methylsulfate, $[C_1Qui][C_1SO_4]$; *N,N*-dimethyl-L-proline methyl ester iodide, $[C_1C_1C_1Pro]I$; *N,N*-dimethyl-L-proline methyl ester methylsulfate, $[C_1C_1C_1Pro][C_1SO_4]$; *N,N*-diethyl-L-proline ethyl ester bromide, $[C_2C_2C_2Pro]Br$; *N,N,N*-trimethyl-L-valinolium iodide, $[C_1C_1C_1Val]I$; and *N,N,N*-trimethyl-L-valinolium methylsulfate,

$[C_1C_1C_1Val][C_1SO_4]$. For the synthesis of the cationic chiral ILs, the reagents used were the quinine (purity = 98 wt%), iodomethane (purity = 99 wt%), dimethyl sulfate (purity = 99 wt%), dichloromethane anhydrous (purity = 99.8 wt%), ethanol (purity = 99.8 wt%), acetone (HPLC grade), potassium carbonate (purity = 99 wt%), L-proline (purity = 99 wt%), bromoethane (purity = 98 wt%), acetonitrile (purity = 99.8 wt%), chloroform (purity = 99 wt%), tetrahydrofuran anhydrous (purity= 99.9 wt%), L-valine (purity = 98 wt%), sodium borohydride (purity = 99 wt%), sulfuric acid (purity = 99.9 wt%), methanol (purity = 99 wt%), ethyl acetate (purity = 99.8 wt%), potassium hydroxide (purity = 90 wt%), formic acid (purity = 98 wt%), formaldehyde (37 wt% in water solution) and hydrochloric acid (37 wt% in water solution) acquired from Sigma-Aldrich. The enantiomers used to perform the precipitation studies were (*R*)-(-)-mandelic acid, *R*-MA (purity = 99 wt%), and (*S*)-(+)-mandelic acid, *S*-MA (purity = 99 wt%), both supplied by Acros Organics. Figure 1 shows the chemical structures and abbreviations of the chiral ILs and mandelic acid enantiomers.

The mobile phase employed in the HPLC-DAD quantification of mandelic acid enantiomers was prepared using copper (II) sulphate pentahydrate, $CuSO_4 \cdot 5H_2O$ (purity > 98 wt%), L-phenylalanine, L-Phe (purity > 98 wt%), respectively purchased from AnalaR and Sigma-Aldrich, methanol (HPLC grade) and ammonia solution at 5% both acquired from CHEM-LAB. The water used for the HPLC analysis was ultra-pure water, double distilled and then treated with a Milli-Q plus 185 water purification apparatus. Syringe filters (0.45 μm) and regenerated cellulose membrane filters (0.45 μm), acquired at Specanalitica and Sartorius, respectively, were used during filtration steps.

For the NMR analysis it was used deuterium oxide, D_2O (purity = 99.9 wt%) and 3-(Trimethylsilyl)propionic-2,2,3,3-D4 acid sodium salt, D 98%, TSP (purity = 99 wt%) both supplied by Eurisotop.

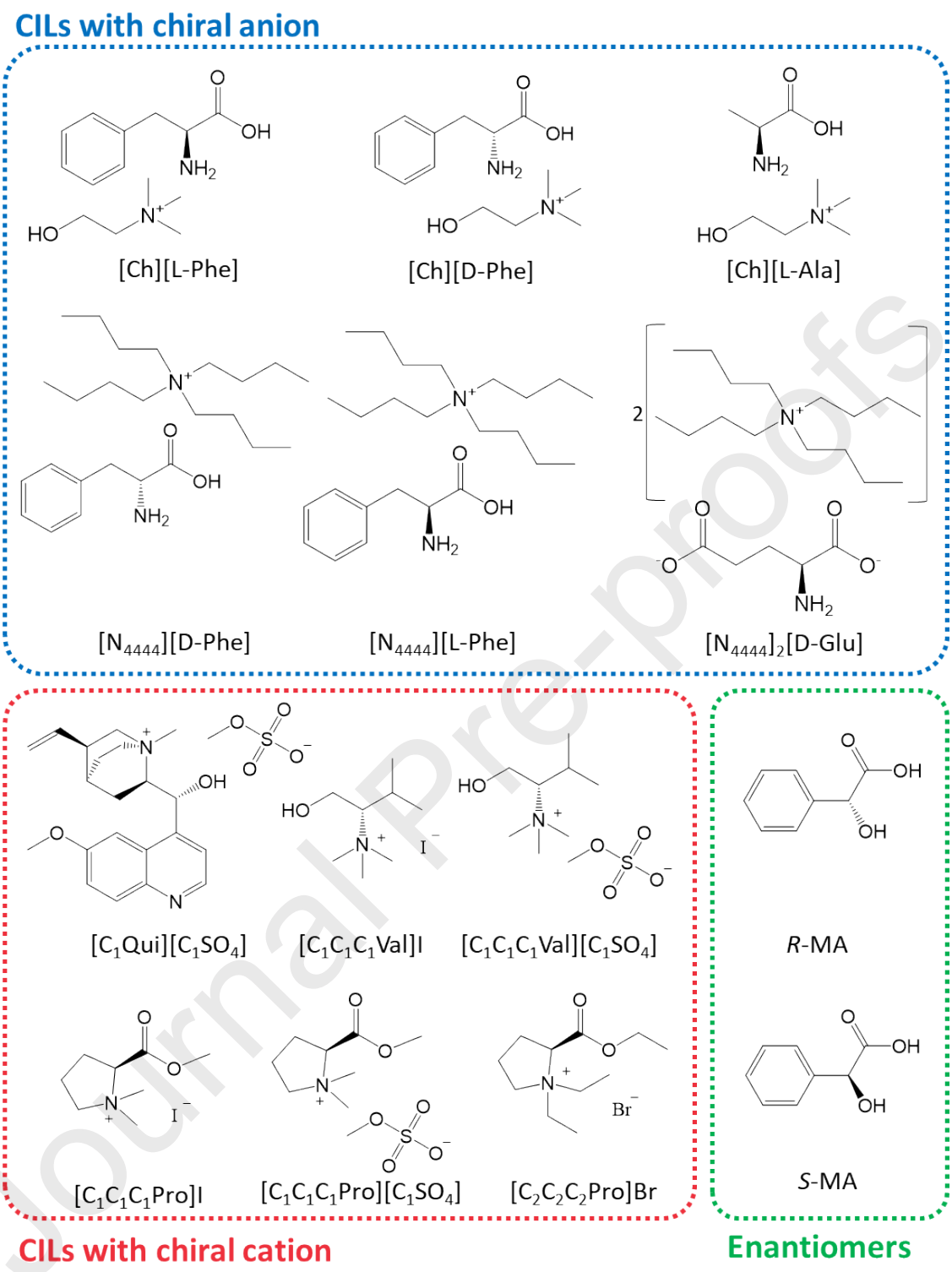

Figure 1. Chemical structures and abbreviations of the chiral ILs (CILs) and mandelic acid (MA) enantiomers investigated in this work.

Experimental

Synthesis of chiral ILs

All chiral ILs were synthesized in our laboratory following well-established protocols.[37–39] The synthesis of the ILs bearing chirality on the anion was achieved through a neutralization reaction occurred by reacting [Ch][OH] or [N_{4444}][OH] with the respective precursor, namely D- and L-Phe, L-Ala and L-Glu. Literature procedures were followed for the synthesis of [N_{4444}]-based-[37] and [Ch]-based chiral ILs.[38] The synthesis of the chiral ILs with chiral cations was performed according to a protocol reported by Sintra et al.[39]: (i) an alkylation reaction between dimethyl sulfate and quinine producing [C_1Qui][C_1SO_4]; (ii) a three step synthesis involving the reduction of L-valine, Eschweiler-Clark reaction and *N*-alkylation yielded L-valine-based chiral ILs; and (iii) alkylation reactions between L-proline and iodomethane, bromoethane, or dimethyl sulfate yielding [$C_1C_1C_1$Pro]I, [$C_2C_2C_2$Pro]Br or [$C_1C_1C_1$Pro][C_1SO_4], respectively.

Enantioselective precipitation procedure

The concentration of the chiral ILs and *R*/*S*-mandelic acid aqueous solutions used in the first screening was fixed at 1.64×10^{-4} mol·mL^{-1} and 3.29×10^{-4} mol·mL^{-1}, respectively. The screening of the various chiral ILs was carried out for 1 day, at 20 °C and 15 rpm, as detailed in ESI, Table S1. For that, the systems were gravimetrically prepared (within $\pm10^{-4}$ g) by adding the respective amount of chiral IL to equal amounts of aqueous solutions of *R*-mandelic acid and *S*-mandelic acid prepared at the same concentration to yield the desired final content in the SLBS. The most promising systems were selected for the evaluation of distinct conditions, namely resolution time (0.5-6 days), resolution speed (0-60 rpm), temperature (4-35 ºC), chiral IL content (10-150 mg.mL^{-1}), racemic mandelic acid content (20-100 mg.mL^{-1}), and water content (83.1-95.4 wt%). The overall mixture compositions and conditions are detailed in ESI, Table S2.

Chiral ILs were placed in contact with the enantiomers in aqueous solution for a set amount of time under constant stirring at the desired temperature, to promote the specific interactions between the chiral ILs and the mandelic acid enantiomers, as advised elsewhere.[25,27] After such a period, if a precipitate was formed on the system, it was separated from the liquid phase. The solid and liquid phases were submitted to HPLC-

DAD analysis for mandelic acid enantiomers quantification. To estimate the average enantioseparation parameters and corresponding standard deviations, triplicates were performed. For comparison purposes, the ability of the amino acid precursors L- and D-Phe to induce enantioselective precipitation was addressed by following the same protocol.

To evaluate the enantioselective precipitation performance the enantiomeric excess (*e.e., %*) and yield for each mandelic acid enantiomer ($Yield_{R-MA\,(S-MA)}$, %) in the solid phase were calculated, according to Equations 1 and 2, respectively:

$$e.e.,\,\% = \frac{m_{R-MA\,(S-MA)\,in\,solid} - m_{S-MA\,(R-MA)\,in\,solid}}{m_{R-MA\,in\,solid} + m_{S-MA\,in\,solid}} \times 100 \quad (1)$$

$$Yield_{R-MA\,(S-MA)},\,\% = \frac{m_{R-MA\,(S-MA)\,in\,solid}}{m^{0}_{R-MA\,(S-MA)}} \times 100 \quad (2)$$

where $m_{R-MA\,in\,solid}$ is the mass of *R*-enantiomer present in the solid phase. $m_{S-MA\,in\,solid}$ is the mass of *S*-enantiomer present in the solid phase, $m^{0}_{R-MA\,(S-MA)}$ is the initial mass of *R*-enantiomer or *S*-enantiomer. The enantiomeric excess data is identified as corresponding to a *R*-mandelic acid or *S*-mandelic acid enriched precipitate by assigning the proper enantiomer to the enantiomeric excess value within brackets.

Mandelic acid enantiomers quantification

The quantification of mandelic acid enantiomers was done by HPLC-DAD using an analytical method adapted from Yue et al.[40] and previously validated by us.[25] The liquid chromatograph HPLC Elite LaChrom (VWR Hitachi) used was composed of a diode array detector (DAD) l-2455, column oven l-2300, auto-sampler l-2200 and pump l-2130. The analytical column used was purchased from Merck and was constituted by a sorbent LiChrospher 100 RP-18 (5µm) and cartridge LiChroCART 250-4 HPLC-Cartridge, connected to a 5 µm, 4 mm × 4 mm guard column containing the same stationary phase. 22 °C and 25 °C were the temperatures at which the column oven and the autosampler operated, respectively. The mobile phase composition was as follows: methanol:water [15:85 (v/v)] containing 2 mM of L-Phe and 1 mM of $CuSO_4$ at pH 4.00 (±0.01) adjusted by adding an ammonia aqueous solution at 5 wt%. The mobile phase was then filtered under vacuum using regenerated cellulose membrane filters (0.45 µm)

and degassed in an ultrasound bath. The chromatographic separation was carried out under an isocratic elution with a flow-rate of 0.8 $mL \cdot min^{-1}$ and the injection volume was 20 µL. The quantification of mandelic acid enantiomers was performed at 270 nm, resorting to calibration curves previously established. Retention times of both enantiomers differ, with *R*-mandelic acid eluting first at approximately 11.7 min followed by *S*-mandelic acid at circa 13.2 min. The SLBS phases were diluted using water:methanol [85:15 (v/v)] and filtered using syringe filters (0.45 µm). Each sample was injected at least twice.

Characterization of the precipitates by ^{1}H-NMR

The ^{1}H NMR spectra were obtained to characterize the precipitate formed in the $[N_{4444}]$[D-Phe]-based SLBS. For that, the solid phase was dissolved in D_2O and TSP, as the internal reference. The ^{1}H NMR measurements were performed on a Bruker Avance 300 spectrometer operating at 300.13 MHz.

Characterization of the precipitates by single crystal X-ray diffraction

Single crystal X-ray diffraction of the precipitate formed in the [Ch][L-Phe]-based SLBS was done following the procedure described by Maximo et al.,[41] collected on a Bruker D8 Quest photon 100 CMOS diffractometer at -93.15 °C using graphite-monochromatic Mo-K_α radiation (0.71073Å). Data reduction was carried out using the SAINT-Plus software package.[42] Multi-scan absorption correction was applied to all intensity data using the SADABS program.[43] The structure was refined *via* full matrix least squares on F^2 using the SHELX-2014 suite.[44] All non-hydrogen atoms were refined with anisotropic thermal parameters. The C-H hydrogen atoms were included in the structure factor calculations in geometrically idealized positions with isotropic thermal displacements depending on the parent atom, using a riding model. The hydrogen atoms bonded to oxygen and nitrogen atoms were obtained from the last final difference Fourier map. Molecular diagrams were drawn with Olex2 software.[45] The single cell unit parameters are detailed in ESI, Crystal details.

Results and discussion

Evaluating the impact of chiral ILs structures in enantioselective precipitation

To create a versatile platform for enantiomeric resolution, the ability of different chiral ILs to promote the selective precipitation of mandelic acid enantiomers was carefully evaluated. With this aim, twelve chiral ILs, namely $[C_1Qui][C_1SO_4]$, $[C_1C_1C_1Pro]I$, $[C_2C_2C_2Pro]Br$, $[C_1C_1C_1Pro][C_1SO_4]$, $[C_1C_1C_1Val]I$ and $[C_1C_1C_1Val][C_1SO_4]$ bearing chirality on the cation and $[N_{4444}]$[L-Phe], $[N_{4444}]$[D-Phe], [Ch][L-Phe], [Ch][D-Phe], [Ch][L-Ala] and $[N_{4444}]_2$[L-Glu] with chiral anions, were screened under similar conditions as detailed in ESI, Table S1. This set of systems was prepared in order to obtain a stoichiometric proportion between chiral IL and racemic mandelic acid of 1:2, ([MA] = 3.29×10^{-4} mol·mL^{-1}, [CIL] = 1.64×10^{-4} mol·mL^{-1}). By adding an equimolar equivalent amount of chiral IL and of one of the mandelic acid enantiomers, specific interactions could be strategically induced.

Of the selected chiral ILs, only those containing Phe as anion are able to promote the precipitation of mandelic acid, as shown in Table S1 in ESI. Taking these results into account, both Phe precursors were tested individually for comparison. The enantiomeric excess values were calculated, and the data is shown in Figure 2 (and detailed in Table S3 from ESI). The results indicate that L-Phe is more prone to precipitate *S*-mandelic acid, while *R*-mandelic acid is more easily precipitated by the D-Phe, in accordance with the literature.[46,47] Regardless of the cation, i.e., $[Ch]^+$ or $[N_{4444}]^+$, the same enantiorecognition profile is observed for the Phe-based chiral ILs. The chiral ILs-based SLBS exhibit higher enantioselectivities for the solid phase than the amino acids, under the conditions adopted in this work (cf. Figure 2). Moreover, $[N_{4444}]$-based chiral ILs display the highest enantiomeric excess values, of 51%, being more effective than [Ch]-based ones. As it will be discussed into detail below, the presence of an aromatic ring in the anion ($[Phe]^-$ *versus* $[Ala]^-$ *versus* $[Glu]^-$ (cf. Figure 1) along with more hydrophobic cations ($[N_{4444}]^+$ *versus* $[Ch]^+$) plays a key role in the enantioselective precipitation of mandelic acid induced by these chiral ILs in SLBS.

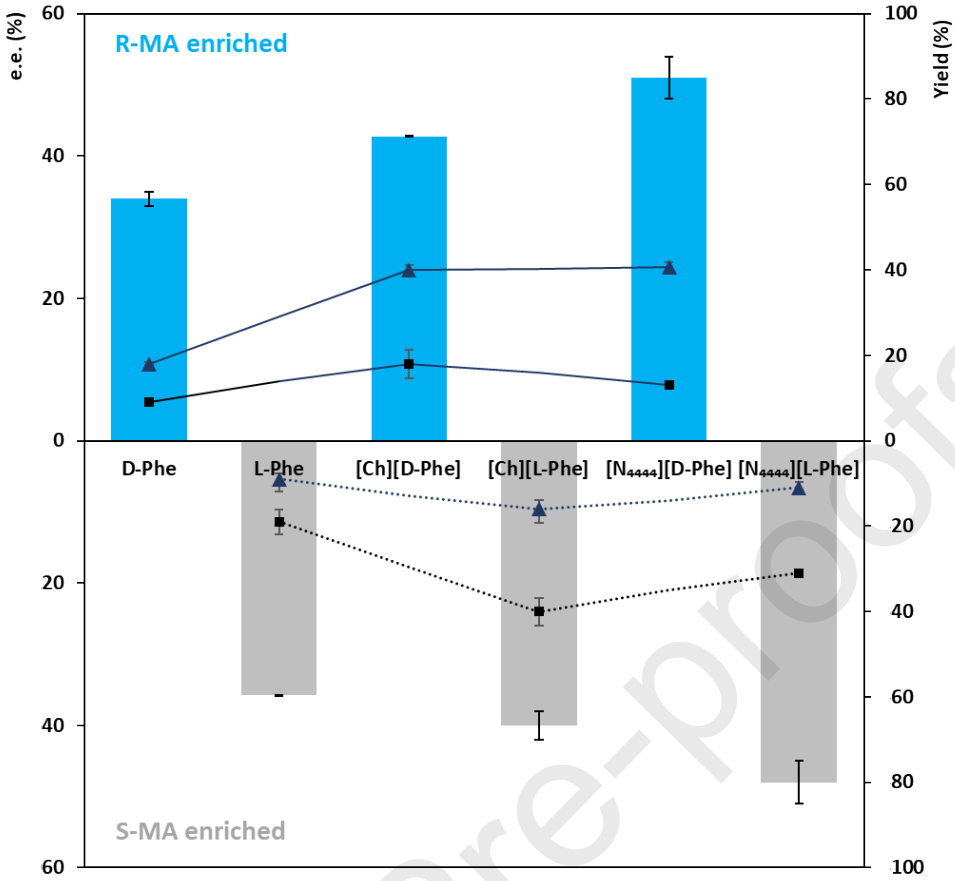

Figure 2. Enantiomeric excesses (*e.e.*, %) and yields of precipitation for either target enantiomer plus the corresponding standard deviations (σ) obtained using SLBS composed of Phe and [Phe]-based chiral ILs: enantiomeric excess for *R*-mandelic acid (blue bars), enantiomeric excess for *S*-mandelic acid (grey bars), $Yield_{R\text{-MA}}$ (blue triangles) and $Yield_{S\text{-MA}}$ (black squares).

Analysis of the precipitate formed

To better understand the composition of the precipitate formed, a NMR analysis was used to characterize the resuspended solid phase obtained with the most enantioselective system, i.e., $[N_{4444}]$[D-Phe]-based SLBS. The results depicted in Figure 3 are indicative of the presence of mandelic acid, chiral IL anion and chiral IL cation in the solid state. The mandelic acid and the chiral IL anion appear at a proportion of 1:1, being the most abundant compounds detected. Approximately, *per* each mandelic acid

molecule, one $[Phe]^-$ molecule is present; whereas the cation concentration is residual, probably resulting from contamination by the liquid phase.

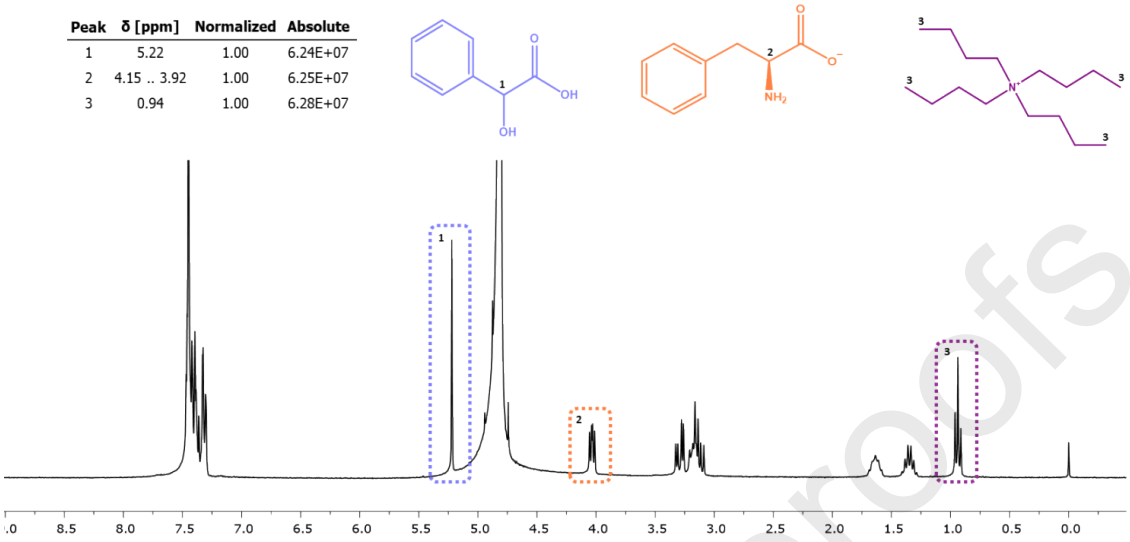

Figure 3. ^{1}H-NMR analysis of the solid phase resuspended after phase separation. The presence of mandelic acid, $[Phe]^-$ and $[N_{4444}]^+$ were estimated from their respective CH, CH and CH_3 peaks at δ=5.22 ppm (1 hydrogen, peak 1), δ=4.03 ppm (1 hydrogen, peak 2) and δ=0.94 ppm (12 hydrogen, peak 3).

Molecular-level mechanisms underlying the enantioselective precipitation phenomenon

The precipitation and enantio-recognition patterns are highly contingent on the chiral IL structure. The principle of enantiomeric recognition for enantioselective complexation follows the "three-point interaction" model, according to which three simultaneous intermolecular interactions take place and lead to the formation of "chiral selector-enantiomer" complexes. Hence, to gain further insight on the interactions occurring between the mandelic acid enantiomers and the chiral ILs, X-Ray diffraction analysis of the solid phases was assessed. Only chiral ILs bearing the $[Ch]^+$ cation could form crystals to be analysed by single crystal X-ray diffraction. Figure 4 corresponds to the results from the analysis of an [L-Phe]:[*S*-mandelic acid] crystal coming from the [Ch][L-Phe]-based SLBS.

The X-ray structure data allowed to confirm that [L-Phe] and *S*-mandelic acid are present in the solid phase. The [L-Phe]:[*S*-mandelic acid] crystal belongs to monoclinic

system with space group C_2, refined as racemic twinning with BASF equal to 0.5315. The crystallographic details of this crystal is given in the experimental part. The asymmetric unit contains one molecule of mandelic acid and one molecule of phenylalanine (Figure 4, left). The carbonyl group of phenylalanine molecule exhibit C-O short distances (C9-O4=1.240(5) and C9-O5=1.267(5) Å). From the Fourier map is not observable any hydrogen atom close to O4 and O5, whereas close to amine group three protons were found. In mandelic acid molecule the distance C1-O2 is 1.293(6) Å and contain a hydrogen bonded which was also taken from the Fourier map. The two molecules [L-Phe] and [*S*-mandelic acid] are assembled into 2-D network (Figure 4, right) of non-covalent interactions like (N-H···O) hydrogen bonding interactions (N1-H1A···O1=2.858(4) Å, N1-H1B···O3=2.875(5) Å, N1-H1C···O5=2.729(5) Å) and (O-H···O) interactions (O2-H2A···O5= 2.534(5) Å, O3-H3···O4 = 2.680(4) Å.

In line with the enantiomeric excess obtained, L-Phe favourably interacts with the *S*-mandelic acid enantiomer, while D-Phe forms more stable complexes with the *R*-mandelic acid enantiomer.

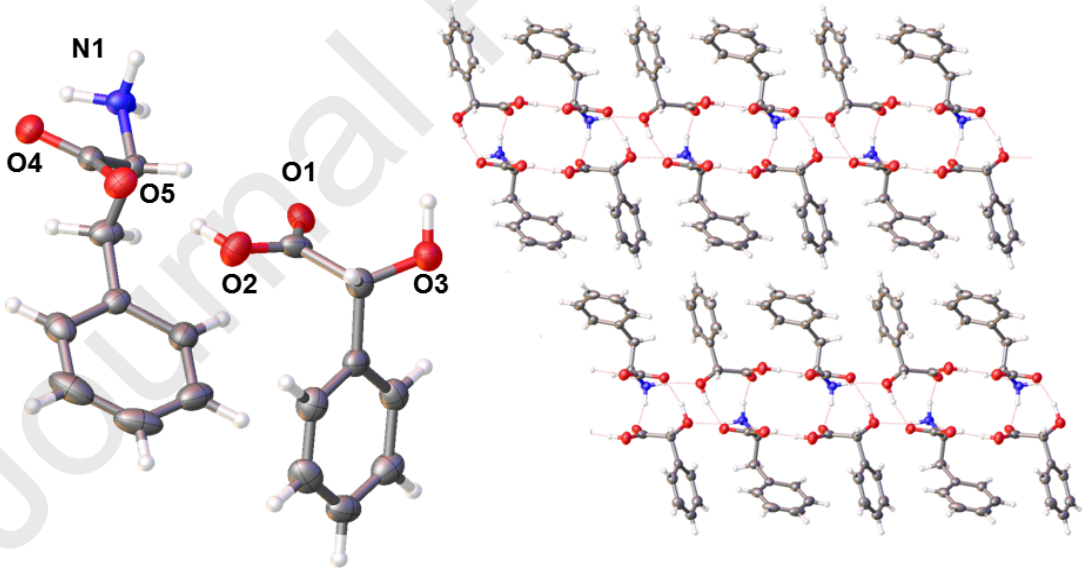

Figure 4. X-ray single crystal structure of L-Phe:*S*-MA showing two different features: left: asymmetric unit; right: crystal packing along b direction assembling the two molecules L-Phe and *S*-mandelic acid through N-H···O and O-H···O hydrogens bonding interactions.

This is in agreement with Guo et al.[48] and can be justified by the solubility of the complexes. The solubility of [L-Phe]:[*S*-mandelic acid] is lower than that of [L-Phe]:[*R*-mandelic acid], implicitly indicating the higher stability of the first complex.[48] Crystallographic studies of diastereomeric crystals performed by Okamura et al.[46] indicate that a common characteristic hydrogen-bond network is formed in [L-Phe]:[*S*-mandelic acid] crystals. The binding forces for this complex are much stronger. Each unit has hydrogen bonds with translational neighboring units, resulting in the formation of a columnar structure which is stable and favorable from the viewpoint of hydrogen bonding interactions (Figure 4B). Meanwhile, [L-Phe]:[*R*-mandelic acid] is less stable, since the hydrogen bond between carboxylate and ammonium was not observed. Okamura describes six kinds of hydrogen bonds but two out of them were bifurcated, thus reducing the interaction strength of its hydrogen bond.[46] The lattice energy and the interaction forces of [L-Phe]:[*R*-mandelic acid] are lower than those of [L-Phe]:[*S*-mandelic acid], thus resulting in its higher solubility.

Comparing the opposite capacity of [Ch][L-Phe] and [Ch][L-Ala] in creating SLBS, it is possible to infer about the amino acid structure influence. Particularly, for these two amino acids, the role of the interactions established due to the presence of the aromatic rings can be asserted. L-Ala shows a similar structure to L-Phe, sharing the same chiral centre, but lacking the presence of an aromatic ring (cf. Figure 1). This indicates that π-π interactions favour the positioning of the chiral centres, promoting their interaction, thus allowing enantiospecific recognition of this aromatic alpha hydroxy acid. It is then possible to infer that a similar reason is behind the inability of $[N_{4444}]_2$[L-Glu] to form a precipitate, since [L-Glu] also lacks an aromatic ring (cf. Figure 1). Additionally, the higher number of cations present, i.e. two exist *per* anion, may lead to a sort of steric hindrance.

The chiral ILs with chiral cation do not promote the enantioselective precipitation of mandelic acid. It is possible that interactions are established between the cation and the negatively charged enantiomer in a selective manner, increasing the solubility of the complex, however, impediments on a structural level may occur. Both for valinolium- and proline-based chiral ILs, the absence of aromatic rings must influence the lack of stability for a macromolecular arrangement. Even though incorporating aromatic rings (cf. Figure 1), the quinine-based chiral IL has a complex structure that may be less likely to promote a stable arrangement with the mandelic acid enantiomer or the solubility of the complex formed is not low enough to induce precipitation.

Optimization studies: evaluating the impact of the operational conditions in enantioselective precipitation

$[N_{4444}][D\text{-Phe}]$ and $[N_{4444}][L\text{-Phe}]$, here identified as the best enantiorecognition agents, were used for further optimization studies to infer on the role of the operational conditions in SLBS performance. The effect of resolution time, resolution speed, resolution temperature, mandelic acid content, chiral IL content and water content was appraised as specified in Table S2 from ESI. The results obtained are depicted in Figure 5 and described in detail in Tables S4-S9 from ESI.

The enantioselective precipitation parameters obtained for $[N_{4444}][D\text{-Phe}]$ and $[N_{4444}][L\text{-Phe}]$ are mirrored in every condition, i.e., $[N_{4444}][D\text{-Phe}]$ exhibits preferable chiral recognition for the *R*- over the *S*- mandelic acid, while $[N_{4444}][L\text{-Phe}]$ establishes stronger interactions with the *S*- over the *R*- mandelic acid. To facilitate the discussion of the results, and since both chiral ILs present the same behaviour, the discussion throughout this work will focus on $[N_{4444}][D\text{-Phe}]$. The body of results collected suggests that the different conditions evaluated affect differently the separation of mandelic acid enantiomers (cf. Figure 5 and Tables S4-S9 from ESI).

Effect of the resolution time

The resolution time can greatly impact the intermolecular interactions between the chiral selector and the target enantiomer. Hence, the effect of resolution time was studied between 0.5 and 6 days and the corresponding results are displayed in Figure 5A and further detailed in Table S4 from ESI. As depicted, no precipitation takes place for periods below 0.5 days. The experimental results indicate that a maximum enantiomeric excess value of 51 ± 3% is achieved after 1 day, followed by a slight decrease of circa 5% up to 6 days. Given the slight decrease of $Yield_{R\text{-MA}}$ (from 40.7 ± 0.5% to 38.1 ± 0.9%) and maintenance of $Yield_{S\text{-MA}}$ at around 13-14%, there may be a gradual loss of *R*-enantiomer into the liquid phase. Moreover, it may be possible to infer that the [*R*-mandelic acid]:$[N_{4444}][D\text{-Phe}]$ complex is formed prior to the [*S*-mandelic acid]:$[N_{4444}][D\text{-Phe}]$ complex. This may also suggest that the solubility of the [*S*-mandelic acid]:[chiral IL] complex is higher in the liquid phase. This behaviour is in accordance with Huang *et.*

al.[33] Since 1 day was the optimum resolution time, it will be adopted in further optimization studies.

Effect of the resolution speed

The resolution speed can greatly influence the contact between the chiral selector and the target enantiomer and thus, the establishment of intermolecular interactions promoting enantiorecognition. The chiral ILs were placed in contact with the mandelic acid enantiomers in aqueous solution under constant stirring, to promote specific interactions between the chiral IL and the target enantiomers. To this aim, different stirring speeds were tested, namely 0, 15, 30 and 60 rpm. The results depicted in Figure 5B and in Table S5 from ESI attest the significance of this parameter, where non-stirred assays showed the lowest enantiomeric excess (35.8 ± 0.8%), most likely due to the poor contact between chiral IL and the target enantiomer. A speed of 15 rpm, where the molecular motions are slower, seems to favour the interactions between *R*-mandelic acid and [N_{4444}][D-Phe] (*e.e.* = 51 ± 3%), being thus adopted in further optimization studies.

Effect of the temperature

The resolution temperature has a significant effect on the intermolecular interactions between enantiomers and the chiral selector that may affect the enantiomeric excess. The effect of temperature on the chiral resolution of mandelic acid enantiomers was assessed between 4 and 35 ºC, being displayed in Figure 5C and presented in more detail in Table S6 from ESI. A decrease in solubility in the liquid-phase of both mandelic acid enantiomers and [mandelic acid]:[N_{4444}][D-Phe] complexes at the lower temperature, increases in about 50% both $Yield_{R\text{-MA}}$ and $Yield_{S\text{-MA}}$; still, enantiomeric excess values are compromised (*e.e.* = 38 ± 3% at 4ºC *versus e.e.* = 51 ± 3% at 20 ºC). In turn, the solubility of the complex increases as the temperature rises, thus more of the [*R*-mandelic acid]:[N_{4444}][D-Phe] complex is dissolved in the liquid-phase at 35ºC. Therefore, there is a decrease of both enantiomeric excess and yield in the solid-phase between 20 and 35 ºC (cf. Figure 5C). Based on these results, the best temperature condition must provide a balance between the precipitation yield and solubility of the [mandelic acid]:[N_{4444}][D-Phe] complexes in the liquid-phase, here achieved at 20 ºC (*e.e.* = 51 ± 3%).

Effect of initial concentration of racemic mandelic acid

In chiral resolution, the enantioselectivity can be influenced by the initial concentration of racemic mandelic acid. This effect was evaluated within the range of 20 mg·mL^{-1} to 100 mg·mL^{-1}, with the results being depicted in Figure 5D and Table S7 from ESI. The enantiomeric excess reaches the lowest level with the increase of racemic mandelic acid concentration, possibly due to a competitive behaviour between [*R*-mandelic acid]:[chiral IL] and [*S*-mandelic acid]:[chiral IL] (*e.e.* = 27.6 ± 0.8%). Accordingly, the best mandelic acid concentration is 50 mg·mL^{-1}, where the equimolar equivalent amount between one enantiomer and the anion of the chiral IL is met (*e.e.* = 51 ± 3%). As such, the environment established in the systems positively promotes the formation of the solid while favouring specific interactions between the *R*-mandelic acid and [N_{4444}][D-Phe]. Moreover, at a lower mandelic acid concentration of 40 mg·mL^{-1}, low yields were obtained ($Yield_{R\text{-MA}}$ = 31.9 ± 0.9% and $Yield_{S\text{-MA}}$ = 11.8 ± 0.5%). Under these conditions, the water content is higher, meaning that more water molecules are present and free to interact and solubilize mandelic acid enantiomers in the system, overwhelming the intermolecular interactions governing the formation of *R*-MA:[N_{4444}][D-Phe] complexes.

Effect of the initial concentration of CIL

The resolution of the mandelic acid enantiomers is mainly dependent on the competitive formation between the [*R*-mandelic acid]:[chiral IL] and [*S*-mandelic acid]:[chiral IL] and on the stability of each complex in aqueous solution. Both Figure 5E and Table S8 in ESI show the enantioselective precipitation data as a function of the chiral IL concentration in the system in the range of 10 mg·mL^{-1} to 150 mg·mL^{-1}. The initial fixed condition at 67 mg·mL^{-1} allowed the best enantiomeric excess (of 51 ± 3%), as the amount of chiral IL and one mandelic acid enantiomer is stoichiometrically equivalent. The enantiomeric excess values drop when the chiral IL content increases after this point. The competition between the complexes stops exerting any effect, as there is enough IL to interact with all the present mandelic acid. At concentrations below 67 mg·mL^{-1}, it may be possible that the higher water content is impacting on the SLBS performance, namely

by decreasing the intermolecular interactions that lead to the formation of *R*-MA:[N_{4444}][D-Phe] complexes.

Effect of amount of water

The SLBS performance is related with the amount of water, since it will affect the amount of chiral complex being transferred into the solid-phase. Figure 5F and Table S9 from ESI present all gathered data regarding the effect of the amount of water on the enantiomeric excess and yields afforded by the SLBS investigated. With the increase of the water content up to 89.0 wt%, the enantiomeric excess value increases from 25 ± 3% to 51 ± 3%, being followed by a slight decrease down to 40.5 ± 0.6%. This can be attributed to the different stability and solubility of the [*R*-mandelic acid]:[N_{4444}][D-Phe] and [*S*-mandelic acid]:[N_{4444}][D-Phe] complexes. When the amount of water is lower, the solubility of the complexes decreases. Both enantiomeric complexes tend to precipitate, which results in a lower enantiomeric excess and higher yields (cf. Figure 5F). With the increase of the water content, less [*S*-mandelic acid]:[N_{4444}][D-Phe] complex is formed. The most specific interactions established for the [*R*-mandelic acid]:[N_{4444}][D-Phe] complex prevail, enhancing the enantiomeric excess to 51 ± 3%; still, a lower amount of precipitate is formed (cf. Figure 5F).

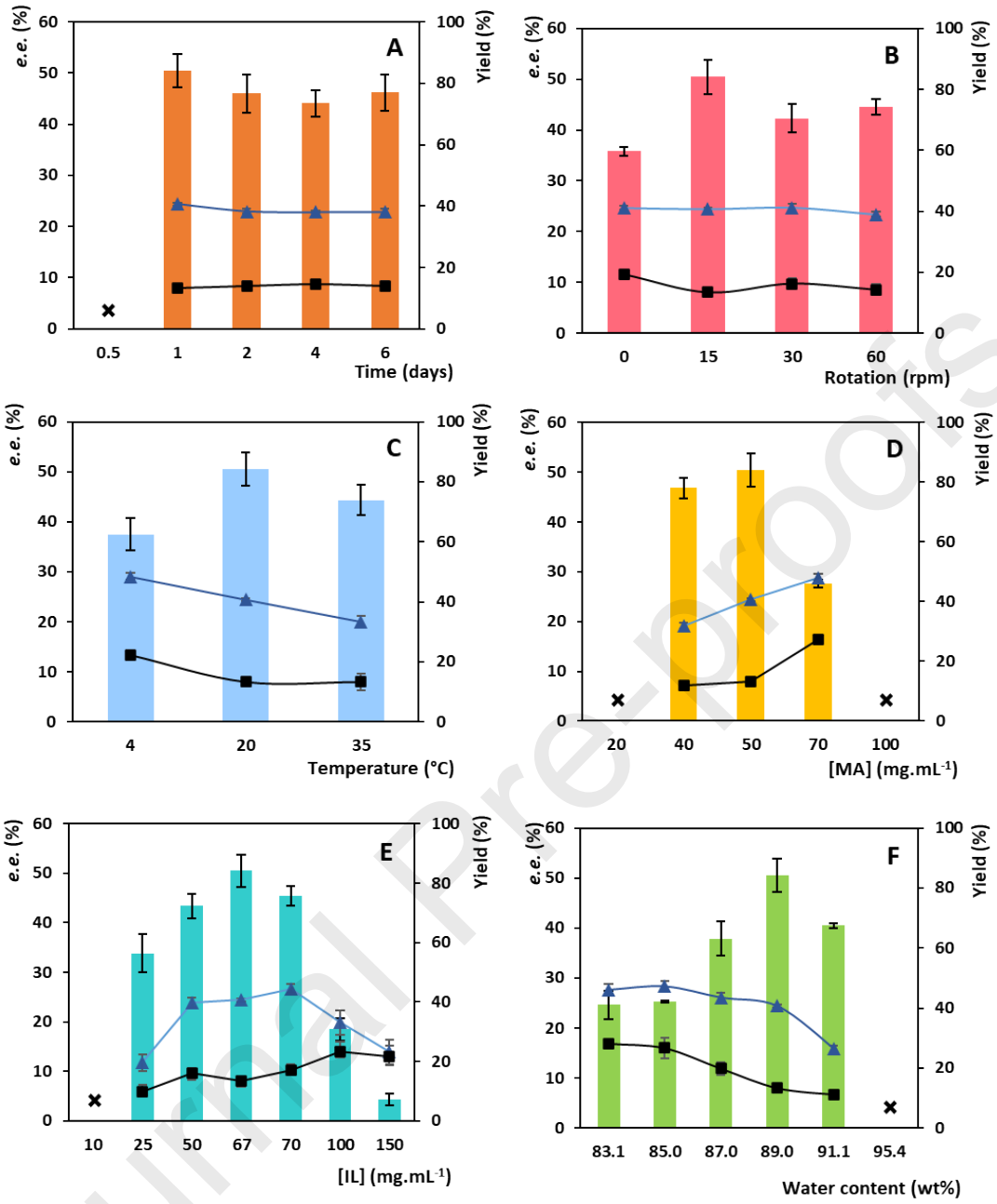

Figure 5. Effect of various operational conditions on the enantiomeric excesses (*e.e.*, bars) and yields of precipitation for either target enantiomer ($Yield_{R\text{-MA}}$, blue triangles and $Yield_{S\text{-MA}}$, black squares) afforded by $[N_{4444}]$[D-Phe]-based SLBS: resolution time (A), resolution speed (B), resolution temperature (C), initial concentration of racemic mandelic acid ([MA] in $mg.L^{-1}$) (D), initial concentration of chiral IL ([CIL] in $mg.L^{-1}$) (E), water content (in wt%) (F). The (x) represents SLBS where a precipitate did not form.

Overall, the body of data gathered allowed us to identify the most important variables to be optimized to create efficient SLBS, while achieving high enantiomeric excesses. Figure 6 enlightens the combined effect of the concentration of both chiral IL and mandelic acid, i.e., two particularly important conditions, in the enantioselective precipitation. Within the range of conditions tested, the highest enantiomeric excesses occur at intermediate concentrations of both mandelic acid (40–50 mg·mL^{-1}) and chiral IL (50–70 mg·mL^{-1}). Outside such a region, the enantioselectivity of the process seems to be compromised. It should be also underlined that at the upper and lower bound of mandelic acid concentration (i.e, 20 and 100 mg·mL^{-1}) no precipitation takes place, despite the progressive increase of chiral IL content at 27.6, 50, 67 mg.mL^{-1}.

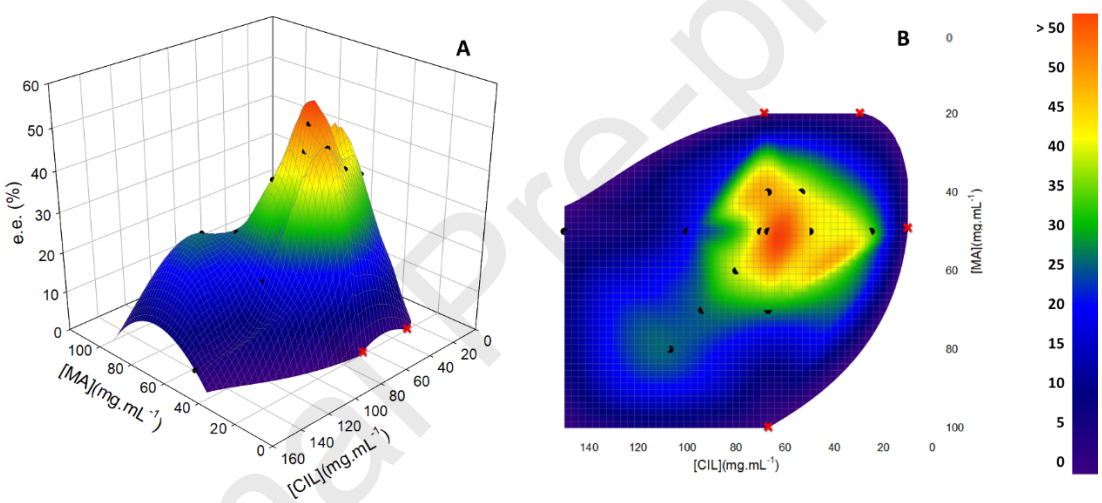

Figure 6. Representation of the combined effect of mandelic acid and chiral IL concentrations towards the enantiomeric excess afforded by [N_{4444}][D-Phe]-based SLBS in 3D (A) and 2D (B): circles (points with formed precipitate); cross (points with no formed precipitate). The surface was drawn with the experimental data obtained and is only a guide to the eye.

Critical assessment of CIL-based SLBS in the development of enantioseparation processes

Numerous chiral IL-based strategies have been explored for enantioseparation purposes. In the light of cost-effectiveness and scalability, several enantioseparation techniques have been reported by exploring the chiral ILs dual function as chiral solvent/chiral selector to develop conventional enantioselective liquid-liquid extractions,[23,24] enantioselective liquid-liquid extractions based on aqueous biphasic systems[25–28] or three-phase partitioning.[28]

Functional amino acid-based chiral ILs were tested as solvents and selectors for the enantioselective liquid-liquid extraction of different racemic amino acids. In those works, the authors opted to use the amino acid-based chiral ILs both as solvent and chiral selector, ethylacetate as a donor phase and copper ion (Cu^{2+}) as a chelant agent. A maximum enantiomeric excess of 50.6 % for Phe was attained,[23] however, the use of both an organic solvent and an additive to promote the enantioseparation compromises the environmental benignity and technological simplicity of the proposed approach. Alternatively, Zgonnik et al.[24] proposed an innovative set of systems called "ILs ion cross-metathesis", where the formation of an IL hydrophobic phase and an aqueous phase takes place. In spite of providing a more benign route for enantioseparations than that of Tang et al.,[23] this strategy is rather constrained by the modest enantioselectivities attained (*e.e.* = 30%) and the limited structural diversity of hydrophobic ILs.[24,32]

To overcome the high environmental burden and lack of technological versatility displayed by enantioselective liquid-liquid extractions, the use of either chiral IL-based aqueous biphasic systems or three-phase partitioning was also considered. Using chiral ILs both as solvent and chiral selectors in aqueous biphasic systems, technologically flexible techniques were created; yet, with maximum enantiomeric excess of 53% for Phe[27]and of 17% for mandelic acid attained, their performance is rather modest (particularly with mandelic acid).[25] Instead using chiral IL-based three-phase partitioning systems, tropine-like chiral ILs were employed for the resolution of racemic amino acids. These systems build up on the formation of two liquid phases and a solid interphase where the target amino acid enantiomer is enriched with a enantiomeric excess of around 80%.[28]

Given the need for extra components displayed by chiral IL-based aqueous biphasic systems and three-phase partitioning, most often a salting-out species and a

coordination agent,[23,26,28] chiral IL-based SLBS can be envisaged as simpler and quicker tools for enantioseparations.[33–36] So far, some authors reported remarkable enantiomeric excess of 99% (for L-Phe); yet, most of these strategies rely on copper salts as coordination agents to boost enantioselectivity.[33–35] As shown in Figure 6, the chiral IL-based SLBS herein developed contribute to improve the degree of operational simplicity of enantioseparations, since by simply using a chiral IL aqueous solution a enantiomeric excess of circa 50% was accomplished for mandelic acid.

Figure 7. Schematic representation of the chiral separation of mandelic acid enantiomers using a chiral IL-based SLBS: chiral IL (yellow hexagon), *R*- mandelic acid (pink square), *S*- mandelic acid (green circle).

Conclusions

In the search for alternative techniques for the resolution of racemic mixtures, chiral ILs were proposed as chiral selectors in SLBS to separate the enantiomers of mandelic acid. An initial screening comprising six chiral IL bearing chirality on the anion and five chiral ILs with chiral cations was performed. This allowed to evaluate their aptitude to form *R*- or *S*-MA:CIL complexes and selectively precipitate mandelic acid enantiomers. Among the distinct chiral ILs evaluated, only those incorporating chiral anions, in particular [L-Phe]$^-$ or [D-Phe]$^-$, were prone to induce mandelic acid precipitation. These were then

subjected to detailed optimization, comprising the following parameters: resolution time, resolution speed, temperature, mandelic acid content, chiral IL content and water content. The chiral IL structure was shown to be paramount to induce the enantiomers precipitation, as further confirmed by ^{1}H NMR and X-ray diffraction studies. The remaining conditions also played a role, with the molar ratio between the mandelic acid enantiomers and chiral IL being critical to the SLBS performance and selectivity. A maximum enantiomeric excess of 51 ± 3% was attained with [N_{4444}][D-Phe] for the selective precipitation of *R*- mandelic acid, and for the selective precipitation of *S*-mandelic acid, a maximum of 48 ± 3% with [N_{4444}][L-Phe]. Without the need of extra additives, as often reported in literature, the chiral IL-based SLBS here proposed offer an extra degree of technological simplicity, moving towards the goal of creating operationally convenient and cost-effective techniques for enantioseparations.

Supplementary material

Electronic Supplementary Information (ESI) available: detailed information of the chiral ILs and operational conditions studied in SLBS; detailed information about the enantiomeric excess and yield of mandelic acid enantiomers; CCDC 1993647 for [L-Phe]:[*S*-MA], contains the supplementary crystallographic data for this paper. Copy of the data can be obtained free of charge on application to CCDC, 12 Union Road, Cambridge CB2 1EZ, UK fax (+44)1223 336033, e-mail: deposit@ccdc.cam.ac.uk

Acknowledgements

This work was developed within the scope of the project CICECO-Aveiro Institute of Materials, UIDB/50011/2020 & UIDP/50011/2020, financed by national funds through the Portuguese Foundation for Science and Technology/MCTES. This work was also financially supported by the project POCI-01-0145-FEDER-030750 (PTDC/EQU-EPQ/30750/2017) - funded by FEDER, through COMPETE2020 - Programa Operacional Competitividade e Internacionalização (POCI), and by national funds (OE), through FCT/MCTES. The NMR spectrometers are part of the National NMR Network (PTNMR) and are partially supported by Infrastructure Project Nº 022161 (co-financed by FEDER

through COMPETE 2020, POCI and PORL and FCT through PIDDAC). M. Kholany acknowledges FCT for the doctoral grant SFRH/BD/138413/2018.

References

[1] G.Q. Lin, J.G. Zhang, J.F. Cheng, Overview of Chirality and Chiral Drugs, in: Chiral Drugs Chem. Biol. Action, John Wiley & Sons, Inc., 2011: pp. 3–28. doi:10.1002/9781118075647.ch1.

[2] M.C. Núñez, M.E. García-Rubiño, A. Conejo-García, O. Cruz-López, M. Kimatrai, M. a Gallo, A. Espinosa, J.M. Campos, Homochiral drugs: a demanding tendency of the pharmaceutical industry., Curr. Med. Chem. 16 (2009) 2064–74. doi:10.2174/092986709788682173.

[3] L.A. Nguyen, H. He, C. Pham-Huy, Chiral drugs: an overview, Int. J. Biomed. Sci. 2 (2006) 85–100. http://www.ncbi.nlm.nih.gov/pubmed/17221858.

[4] FDA'S policy statement for the development of new stereoisomeric drugs, Chirality. 4 (1992) 338–340. doi:10.1002/chir.530040513.

[5] S. Mane, Racemic drug resolution: A comprehensive guide, Anal. Methods. 8 (2016) 7567–7586. doi:10.1039/c6ay02015a.

[6] H.-U. Blaser, Chirality and its implications for the pharmaceutical industry, Rend. Lincei. 24 (2013) 213–216. doi:10.1007/s12210-012-0220-2.

[7] B. Schuur, B.J. V Verkuijl, A.J. Minnaard, J.G. de Vries, H.J. Heeres, B.L. Feringa, Chiral separation by enantioselective liquid-liquid extraction., Org. Biomol. Chem. 9 (2011) 36–51. doi:10.1039/c0ob00610f.

[8] H. Lorenz, A. Seidel-Morgenstern, Processes to separate enantiomers, Angew. Chemie - Int. Ed. 53 (2014) 1218–1250. doi:10.1002/anie.201302823.

[9] Y. Wang, A. Chen, Crystallization-based separation of enantiomers, in: V. Andrushko, N. Andrushko (Eds.), Stereoselective Synth. Drugs Nat. Prod., 1st ed., JohnWiley & Sons, Inc, 2013: pp. 1663–1682.

[10] L.R. Snyder, J.J. Kirkland, J.W. Dolan, Introduction to Moderns Liquid Chromatography, 3rd ed., John Wiley & Sons, Inc., 2010. doi:10.1002/9780470508183.

[11] M.G. Freire, A.F.M. Cláudio, J.M.M. Araújo, J.A.P. Coutinho, I.M. Marrucho, J.N. Canongia Lopes, L.P.N. Rebelo, Aqueous biphasic systems: a boost brought about by using ionic liquids., Chem. Soc. Rev. 41 (2012) 4966–4995. doi:10.1039/c2cs35151j.

[12] M. Freemantle, Designer Solvents: Ionic liquids may boost clean technology development, Chem. Eng. News. 76 (1998) 32–37. doi:10.1021/cen-v076n013.p032.

[13] M.J. Earle, P.B. McCormac, K.R. Seddon, Diels–Alder reactions in ionic liquids, Green Chem. 1 (1999) 23–25. doi:10.1039/a808052f.

[14] V. Kumar, C. Pei, C.E. Olsen, S.J.C. Schäffer, V.S. Parmar, S. V. Malhotra, Novel carbohydrate-based chiral ammonium ionic liquids derived from isomannide, Tetrahedron Asymmetry. 19 (2008) 664–671. doi:10.1016/j.tetasy.2008.02.009.

[15] L. Poletti, C. Chiappe, L. Lay, D. Pieraccini, L. Polito, G. Russo, Glucose-derived ionic liquids: exploring low-cost sources for novel chiral solvents, Green Chem. 9 (2007) 337. doi:10.1039/b615650a.

[16] W. Bao, Z. Wang, Y. Li, Synthesis of Chiral Ionic Liquids from Natural Amino Acids, J. Org. Chem. 68 (2003) 591–593. doi:10.1021/jo020503i.

[17] X. Chen, X. Li, A. Hu, F. Wang, Advances in chiral ionic liquids derived from natural amino acids, Tetrahedron: Asymmetry. 19 (2008) 1–14. doi:10.1016/J.TETASY.2007.11.009.

[18] M. Bonanni, G. Soldaini, C. Faggi, A. Goti, F. Cardona, Novel l -Tartaric Acid Derived Pyrrolidinium Cations for the Synthesis of Chiral Ionic Liquids, Synlett. 2009 (2009) 747–750. doi:10.1055/s-0028-1087950.

[19] T. Heckel, A. Winkel, R. Wilhelm, Chiral ionic liquids based on nicotine for the chiral recognition of carboxylic acids, Tetrahedron Asymmetry. 24 (2013) 1127–1133. doi:10.1016/j.tetasy.2013.07.021.

[20] S. Malhotra, Y. Wang, V. Kumar, α-Pinene-Based New Chiral Ionic Liquids and their Application as Phase Transfer Catalysts in Enantioselective Addition of Diethylzinc to Aldehydes, Lett. Org. Chem. 6 (2009) 264–268. doi:10.2174/157017809787893073.

[21] K. Bica, P. Gaertner, Applications of Chiral Ionic Liquids, European J. Org. Chem. 2008 (2008) 3235–3250. doi:10.1002/ejoc.200701107.

[22] B. Soares, H. Passos, C.S.R. Freire, J.A.P. Coutinho, A.J.D. Silvestre, M.G. Freire, Ionic liquids in chromatographic and electrophoretic techniques: toward additional

improvements in the separation of natural compounds, Green Chem. 18 (2016) 4582–4604. doi:10.1039/C6GC01778A.

[23] F. Tang, Q. Zhang, D. Ren, Z. Nie, Q. Liu, S. Yao, Functional amino acid ionic liquids as solvent and selector in chiral extraction, J. Chromatogr. A. 1217 (2010) 4669–4674. doi:10.1016/J.CHROMA.2010.05.013.

[24] V. Zgonnik, C. Zedde, Y. Génisson, M.R. Mazières, J.C. Plaquevent, Synthesis of chiral ionic liquids by ion cross-metathesis: En route to enantioselective water-ionic liquid extraction (EWILE), an eco-friendly variant of the ELLE process, Chem. Commun. 48 (2012) 3185–3187. doi:10.1039/c2cc17799d.

[25] F.A. e Silva, M. Kholany, T.E. Sintra, M. Caban, P. Stepnowski, S.P.M. Ventura, J.A.P. Coutinho, Aqueous Biphasic Systems Using Chiral Ionic Liquids for the Enantioseparation of Mandelic Acid Enantiomers, Solvent Extr. Ion Exch. 36 (2018) 617–631. doi:10.1080/07366299.2018.1545344.

[26] D. Sun, R. Wang, F. Li, L. Liu, Z. Tan, Enantioselective Extraction of Phenylalanine Enantiomers Using Environmentally Friendly Aqueous Two-Phase Systems, Processes. 6 (2018) 212. doi:10.3390/pr6110212.

[27] D. Wu, Y. Zhou, P. Cai, S. Shen, Y. Pan, Specific cooperative effect for the enantiomeric separation of amino acids using aqueous two-phase systems with task-specific ionic liquids, J. Chromatogr. A. 1395 (2015) 65–72. doi:10.1016/j.chroma.2015.03.047.

[28] H. Wu, S. Yao, G. Qian, T. Yao, H. Song, A resolution approach of racemic phenylalanine with aqueous two-phase systems of chiral tropine ionic liquids, J. Chromatogr. A. 1418 (2015) 150–157. doi:10.1016/j.chroma.2015.09.058.

[29] M. Kowacz, P. Groves, J.M.S.S. Esperança, L.P.N. Rebelo, On the use of ionic liquids to tune crystallization, Cryst. Growth Des. 11 (2011) 684–691. doi:10.1021/cg101061p.

[30] R.A. Judge, S. Takahashi, K.L. Longenecker, E.H. Fry, C. Abad-Zapatero, M.L. Chiu, The Effect of Ionic Liquids on Protein Crystallization and X-ray Diffraction Resolution, Cryst. Growth Des. 9 (2009) 3463–3469. doi:10.1021/cg900140b.

[31] C.C. Weber, a J. Kunov-Kruse, R.D. Rogers, A.S. Myerson, Manipulation of ionic liquid anion-solute-antisolvent interactions for the purification of acetaminophen., Chem. Commun. (Camb). 51 (2015) 4294–7. doi:10.1039/c5cc00198f.

[32] S.P.M. Ventura, F.A. e Silva, M. V. Quental, D. Mondal, M.G. Freire, J.A.P. Coutinho,

Ionic-liquid-mediated extraction and separation processes for bioactive compounds: past, present, and future trends, Chem. Rev. 117 (2017) 6984–7052. doi:10.1021/acs.chemrev.6b00550.

[33] X. Huang, H. Wu, Z. Wang, Y. Luo, H. Song, High resolution of racemic phenylalanine with dication imidazolium-based chiral ionic liquids in a solid-liquid two-phase system, J. Chromatogr. A. 1479 (2017) 48–54. doi:10.1016/J.CHROMA.2016.12.012.

[34] Zhixia Wang, Zhenbo Hou, Shun Yao, Min Lin, Hang Song, A new and recyclable system based on tropin ionic liquids for resolution of several racemic amino acids, Anal. Chim. Acta. 960 (2017) 81–89. doi:10.1016/J.ACA.2017.01.050.

[35] H. Zang, S. Yao, Y. Luo, D. Tang, H. Song, Complex-precipitation using functionalized chiral ionic liquids with L-proline anion and chromatographic analysis for enantioseparation of racemic amino acids, Chirality. 30 (2018) 1182–1194. doi:10.1002/chir.23011.

[36] P. Cai, Z. Gao, X. Yin, Y. Luo, X. Zhao, Y. Pan, Facile enantioseparation and recognition of mandelic acid and its derivatives in self-assembly interaction with chiral ionic liquids, J. Sep. Sci. 42 (2019) 3589–3598. doi:10.1002/jssc.201900584.

[37] C.R. Allen, P.L. Richard, A.J. Ward, L.G.A. van de Water, A.F. Masters, T. Maschmeyer, Facile synthesis of ionic liquids possessing chiral carboxylates, Tetrahedron Lett. 47 (2006) 7367–7370. doi:10.1016/j.tetlet.2006.08.007.

[38] S. De Santis, G. Masci, F. Casciotta, R. Caminiti, E. Scarpellini, M. Campetella, L. Gontrani, Cholinium-amino acid based ionic liquids: a new method of synthesis and physico-chemical characterization, Phys. Chem. Chem. Phys. 17 (2015) 20687–20698. doi:10.1039/C5CP01612F.

[39] T.E. Sintra, M.G. Gantman, S.P.M. Ventura, J.A.P. Coutinho, P. Wasserscheid, P.S. Schulz, Synthesis and characterization of chiral ionic liquids based on quinine, l-proline and l-valine for enantiomeric recognition, J. Mol. Liq. 283 (2019) 410–416. doi:10.1016/J.MOLLIQ.2019.03.084.

[40] Y. Yue, X.-Y. Jiang, J.-G. Yu, K.-W. Tang, Enantioseparation of mandelic acid enantiomers in ionic liquid aqueous two-phase extraction systems, Chem. Pap. 68 (2013) 465–471. doi:10.2478/s11696-013-0467-9.

[41] G.J. Maximo, R.J.B.N. Santos, P. Brandão, J.M.S.S. Esperança, M.C. Costa, A.J.A. Meirelles, M.G. Freire, J.A.P. Coutinho, Generating ionic liquids from ionic solids: An

investigation of the melting behavior of binary mixtures of ionic liquids, Cryst. Growth Des. 14 (2014) 4270–4277. doi:10.1021/cg500655s.

[42] Bruker SAINT-plus Bruker AXS Inc.,Madison, Wisconsin, USA, 2007, (n.d.). .

[43] C.A. Anosike, O.N. Igboegwu, O.F.C. Nwodo, Antioxidant properties and membrane stabilization effects of methanol extract of Mucuna pruriens leaves on normal and sickle erythrocytes, J. Tradit. Complement. Med. 9 (2018) 1–7. doi:10.1016/j.jtcme.2017.08.002.

[44] G.M. Sheldrick, SHELX Version 2014/7, (n.d.).

[45] O. V. Dolomanov, L.J. Bourhis, R.J. Gildea, J.A.K. Howard, H. Puschmann, OLEX2: A complete structure solution, refinement and analysis program, J. Appl. Crystallogr. 42 (2009) 339–341. doi:10.1107/S0021889808042726.

[46] K. Okamura, H. Hiramatsu, N. Nishimura, Instrumental Achievements Crystal Structures of Diastereomeric 1 : 1 Complexes of (R) - and (S) -Phenylalanine (S) -Mandelic Acid, 13 (1997).

[47] X.-H. Pham, J.-M. Kim, S.-M. Chang, I. Kim, W.-S. Kim, Enantioseparation of D/L-mandelic acid with L-phenylalanine in diastereomeric crystallization, J. Mol. Catal. B Enzym. 60 (2009) 87–92. doi:10.1016/J.MOLCATB.2008.12.023.

[48] H.S. Guo, J.M. Kim, X.H. Pham, S.M. Chang, W.S. Kim, Predicting the enantioseparation efficiency of chiral mandelic acid in diastereomeric crystallization using a quartz crystal microbalance, Cryst. Growth Des. 11 (2011) 53–58. doi:10.1021/cg100275v.

Supporting Information

Separation of mandelic acid enantiomers using solid-liquid biphasic systems based on chiral ionic liquids

Mariam Kholany[1], Francisca A. e Silva[1], Tânia E. Sintra[1], Paula Brandão[1], Sónia P. M. Ventura[1], João A. P. Coutinho[1]*

[1]CICECO - Aveiro Institute of Materials, Department of Chemistry, University of Aveiro, 3810-193 Aveiro, Portugal

*Corresponding author – E-mail address: jcoutinho@ua.pt (J. A. P. Coutinho)

Table S1. Overview of the different chiral ILs-based SLBS screened to form a precipitate in the enantioseparation of mandelic acid.

Study	Time (days)	Speed (rpm)	Temperature (°C)	[MA], [CIL] (mol·mL^{-1}), (mol·mL^{-1})	Water content (wt%)	Precipitate
Chiral IL with chiral cation						
$[C_1Qui][C_1SO_4]$	1	15	20	(3.29×10^{-4}), (1.64×10^{-4})	89.0	Not formed
$[C_1C_1C_1Pro]I$						Not formed
$[C_2C_2C_2Pro]Br$						Not formed
$[C_1C_1C_1Pro][C_1SO_4]$						Not formed
$[C_1C_1C_1Val]I$						Not formed
$[C_1C_1C_1Val][C_1SO_4]$						Not formed
Chiral IL with chiral cation						
$[N_{4444}]_2$[L-Glu]	1	15	20	(3.29×10^{-4}), (1.64×10^{-4})	89.0	Not formed
[Ch][L-Ala]						Not formed
$[N_{4444}]$[L-Phe]						Formed
$[N_{4444}]$[D-Phe]						Formed
[Ch][L-Phe]						Formed
[Ch][D-Phe]						Formed
Aminoacids						
L-Phe	1	15	20	(3.29×10^{-4}), (1.64×10^{-4})	89.0	Formed
D-Phe						Formed

Table S2. Overall set of conditions evaluated and approximate mixture compositions used in the enantioseparation of mandelic acid with chiral IL-based SLBS.

Study	Time (days)	Speed (rpm)	Temperature (°C)	[MA], [CIL] ($mg \cdot mL^{-1}$), ($mg \cdot mL^{-1}$)	Water content (wt%)
Optimization study – [N_{4444}][L-Phe], [N_{4444}][D-Phe]					
Time	0.5, 1, 2, 3, 4, 5, 6	15	20	50, 67	89.0
Speed	1	0, 15, 30, 60	20	50, 67	89.0
Temperature	1	15	4, 20, 35	50 67	89.0
[MA]	1	15	20	(20, 67), (40, 67), (50, 67), (70, 67), (100, 67)	95.4, 91.1, 89.0, 85.0, 79.4
[IL]	1	15	20	(50, 10), (50, 25), (50, 67), (50, 70), (50, 100), (50, 150)	94.0, 92.7, 89.0, 88.8, 86.4, 82.6
Water content	1	15	20	(20, 27.6), (40, 53.4), (50, 67), (60, 80), (70, 94), (80, 107)	95.4, 91.1, 89.0, 87.0, 85.0, 83.1

Table S3. Enantiomeric excesses (*e.e.*, %) plus the corresponding standard deviations (σ) obtained using SLBS composed of Phe and [Phe]-based chiral ILs. (*R*-MA) and (*S*-MA) indicate the mandelic acid enantiomer in which the formed precipitate is enriched.

Chiral Selector	***e.e.* ± σ (%)**	**Yield $_{R\text{-MA}}$ ± σ (%)**	**Yield $_{S\text{-MA}}$ ± σ (%)**
D-Phe	34 ± 1 (*R*-MA)	18.0 ± 0.5	9.0 ± 0.3
L-Phe	35.8 ± 0.1 (*S*-MA)	9 ± 1	19 ± 3
[Ch][D-Phe]	42.74 ± 0.08 (*R*-MA)	40 ± 3	18 ± 1
[Ch][L-Phe]	40 ± 2 (*S*-MA)	16 ± 2	40 ± 3
[N_{4444}][D-Phe]	51 ± 3 (*R*-MA)	40.7 ± 0.5	13 ± 1
[N_{4444}][L-Phe]	48 ± 3 (*S*-MA)	11 ± 1	31.0 ± 0.3

Table S4. Impact of resolution time in the enantiomeric excesses (*e.e., %*) and yields of precipitation for either target enantiomer ($Yield_{R\text{-MA}}$ and $Yield_{S\text{-MA}}$) plus the corresponding standard deviations (σ) obtained using chiral IL-based SLBS. (*R*-MA) and (*S*-MA) indicate the mandelic acid enantiomer in which the formed precipitate is enriched.

Time (days)	*e.e.* ± σ (%)	Yield $_{R\text{-MA}}$ ± σ (%)	Yield $_{S\text{-MA}}$ ± σ (%)
[N_{4444}][D-Phe]			
0.5	-	-	-
1	51 ± 3 (*R*-MA)	40.7 ± 0.5	13 ± 1
2	46 ± 4 (*R*-MA)	38.3 ± 0.8	14 ± 2
4	44 ± 3 (*R*-MA)	38.0 ± 0.3	14.0 ± 0.9
6	46 ± 4 (*R*-MA)	38.1 ± 0.9	14 ± 2
[N_{4444}][L-Phe]			
0.5	-	-	-
1	48 ± 3 (*S*-MA)	11 ± 1	31.0 ± 0.3
2	44 ± 1 (*S*-MA)	12.8 ± 0.3	32.2 ± 0.5
4	42 ± 4 (*S*-MA)	13 ± 2	31 ± 1
6	45 ± 3 (*S*-MA)	11 ± 1	30 ± 1

Table S5. Impact of resolution speed in the enantiomeric excesses (*e.e.*, %) and yields of precipitation for either target enantiomer ($Yield_{R\text{-MA}}$ and $Yield_{S\text{-MA}}$) plus the corresponding standard deviations (σ) obtained using chiral IL-based SLBS. (*R*-MA) and (*S*-MA) indicate the mandelic acid enantiomer in which the formed precipitate is enriched.

Speed (RPM)	*e.e.* ± σ (%)	Yield $_{R\text{-MA}}$ ± σ (%)	Yield $_{S\text{-MA}}$ ± σ (%)
[N_{4444}][D-Phe]			
0	35.8 ± 0.8 (*R*-MA)	41.0 ± 0.6	19.2 ± 0.7
15	51 ± 3 (*R*-MA)	40.7 ± 0.5	13 ± 1
30	42 ± 3 (*R*-MA)	41 ± 1	16 ± 2
60	45 ± 2 (*R*-MA)	39.1 ± 0.9	14 ± 2
[N_{4444}][L-Phe]			
0	39 ± 1 (*S*-MA)	11 ± 3	26 ± 8
15	48 ± 3 (*S*-MA)	11 ± 1	31.0 ± 0.3
30	47 ± 3 (*S*-MA)	11 ± 1	29.7 ± 0.4
60	46 ± 2 (*S*-MA)	11 ± 1	30 ± 2

Table S6. Impact of resolution temperature in the enantiomeric excesses (*e.e.*, %) and yields of precipitation for either target enantiomer ($Yield_{R\text{-MA}}$ and $Yield_{S\text{-MA}}$) plus the corresponding standard deviations (σ) obtained using chiral IL-based SLBS. (*R*-MA) and (*S*-MA) indicate the mandelic acid enantiomer in which the formed precipitate is enriched.

Temperature (ºC)	***e.e.* ± σ (%)**	**Yield $_{R\text{-MA}}$ ± σ (%)**	**Yield $_{S\text{-MA}}$ ± σ (%)**
[N_{4444}][D-Phe]			
4	37 ± 3 (*R*-MA)	48 ± 1	22 ± 2
20	51 ± 3 (*R*-MA)	40.7 ± 0.5	13 ± 1
35	44 ± 3 (*R*-MA)	33 ± 2	13 ± 3
[N_{4444}][L-Phe]			
4	40 ± 1 (*S*-MA)	17.0 ± 0.4	40 ± 2
20	48 ± 3 (*S*-MA)	11 ± 1	31.0 ± 0.3
35	38 ± 4 (*S*-MA)	9 ± 1	37 ± 2

Table S7. Impact of the initial racemic mandelic acid concentration ([MA] in $mg.mL^{-1}$) in the enantiomeric excesses (*e.e.*, %) and yields of precipitation for either target enantiomer ($Yield_{R\text{-MA}}$ and $Yield_{S\text{-MA}}$) plus the corresponding standard deviations (σ) obtained using chiral IL-based SLBS. (*R*-MA) and (*S*-MA) indicate the mandelic acid enantiomer in which the formed precipitate is enriched.

[MA] ($mg \cdot mL^{-1}$)	***e.e.* ± σ (%)**	**Yield $_{R\text{-MA}}$ ± σ (%)**	**Yield $_{S\text{-MA}}$ ± σ (%)**
[N_{4444}][D-Phe]			
20	-	-	-
40	47 ± 2 (*R*-MA)	31.9 ± 0. 9	11.8 ± 0.5
50	51 ± 3 (*R*-MA)	40.7 ± 0.5	13 ± 1
70	27.6 ± 0.8 (*R*-MA)	48 ± 1	27.3 ± 0.9
100	-	-	-
[N_{4444}][L-Phe]			
20	-	-	-
40	46 ± 1 (*S*-MA)	9 ± 1	27 ± 2
50	48 ± 3 (*S*-MA)	11 ± 1	31.0 ± 0.3
70	40 ± 2 (*S*-MA)	17 ± 2	39 ± 1
100	-	-	-

Table S8. Impact of the initial chiral IL concentration ([CIL] in $mg.mL^{-1}$) in the enantiomeric excesses (*e.e.*, %) and yields of precipitation for either target enantiomer ($Yield_{R\text{-MA}}$ and $Yield_{S\text{-MA}}$) plus the corresponding standard deviations (σ) obtained using chiral IL-based SLBS. (*R*-MA) and (*S*-MA) indicate the mandelic acid enantiomer in which the formed precipitate is enriched.

[CIL] (mg□mL^{-1})	***e.e.* ± σ (%)**	**Yield $_{R\text{-MA}}$ ± σ (%)**	**Yield $_{S\text{-MA}}$ ± σ (%)**
[N_{4444}][D-Phe]			
10	-	-	-
25	34 ± 4 (*R*-MA)	20 ± 3	10 ± 2
50	43 ± 2 (*R*-MA)	40 ± 2	16 ± 2
67	51 ± 3 (*R*-MA)	40.7 ± 0.5	13 ± 1
70	45 ± 2 (*R*-MA)	45 ± 1	17 ± 2
100	18 ± 2 (*R*-MA)	33 ± 4	23 ± 3
150	4 ± 1 (*R*-MA)	23 ± 4	22 ± 4
[N_{4444}][L-Phe]			
10	-	-	-
25	38.6 ± 0.5 (*S*-MA)	6 ± 2	14 ± 3
50	44 ± 1 (*S*-MA)	12 ± 0.3	32 ± 1
67	48 ± 3 (*S*-MA)	11 ± 1	31.0 ± 0.3
70	42 ± 1 (*S*-MA)	15 ± 2	37 ± 4
100	0.8 ± 0.7 (*R*-MA)	9 ± 3	9 ± 2
150	1 ± 1 (*R*-MA)	7.9 ± 0.4	7.8 ± 0.3

Table S9. Impact of the water content (in wt%) in the enantiomeric excesses (*e.e.*, %) and yields of precipitation for either target enantiomer ($Yield_{R\text{-MA}}$ and $Yield_{S\text{-MA}}$, %) plus the corresponding standard deviations (σ) obtained using chiral IL-based SLBS. (*R*-MA) and (*S*-MA) indicate the mandelic acid enantiomer in which the formed precipitate is enriched.

Water content (wt%)	***e.e.*** **± σ (%)**	**Yield $_{R\text{-MA}}$ ± σ (%)**	**Yield $_{S\text{-MA}}$ ± σ (%)**
[N_{4444}][D-Phe]			
83.1	25 ± 3 (*R*-MA)	46 ± 2	28 ± 1
85.0	25.3 ± 0.2 (*R*-MA)	47 ± 2	27 ± 3
87.0	38 ± 4 (*R*-MA)	44 ± 2	20 ± 2
89.0	51 ± 3 (*R*-MA)	40.7 ± 0.5	13 ± 1
91.1	40. 5 ± 0.5 (*R*-MA)	26 ± 1	11 ± 0.5
95.4	-	-	-
[N_{4444}][L-Phe]			
83.1	29 ± 2 (*S*-MA)	27 ± 2	50.3 ± 0.2
85.0	32 ± 3 (*S*-MA)	23 ± 1	45 ± 2
87.0	37 ± 3 (*S*-MA)	24 ± 1	52 ± 1
89.0	48 ± 3 (*S*-MA)	11 ± 1	31.0 ± 0.3
91.1	44 ± 4 (*S*-MA)	7. 9 ± 0.6	20.1 ± 0.9
95.4	-	-	-

Crystal details:

Crystal data of [L-Phe]:[*S*-MA]: $C_{17}H_{19}NO_5$, Mr = 317.33, monoclinic, space group C_2, Z = 4, a = 19.2575(15), b = 5.7192(4), c = 15.6172(13) Å, V = 1553.6(2) Å^3, β = 115.414 (3)º, ρ(calc) = 1.357 Mg m-3, μ= 0.100 mm-1. 12144 reflections were collected and subsequently merged to 2926 unique reflections with a R_{int} of 0.0416. The final refinement of 237 parameters converged to final *R* and R_w indices R_1 = 0.0521 and wR_2 = 0.1397 for 2534 reflections with $I>2\sigma(I)$ and R_1 = 0.0621 and wR_2 =0.1479 for all *hkl* data.

Graphical abstract

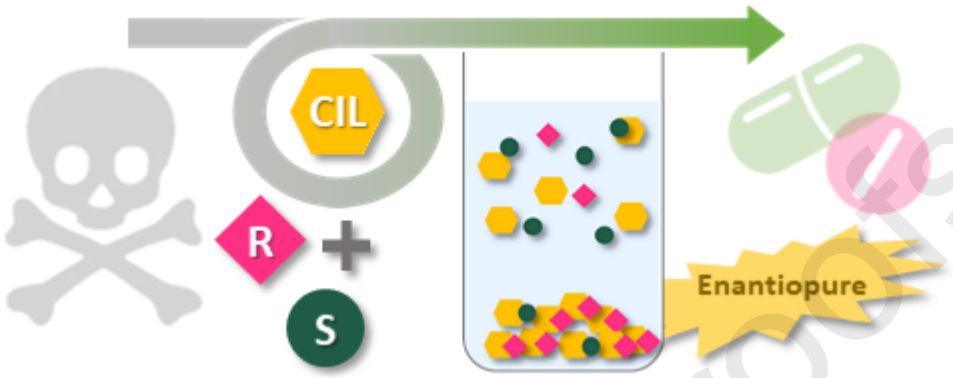

Highlights

- New solid-liquid biphasic systems using chiral ionic liquids are proposed.
- Enantioselective precipitation is used to separate racemic mandelic acid.
- Enantioselective precipitation highly depends on the chiral IL structure.
- Chiral ILs surpass their precursors at inducing enantioselective precipitation.
- $[N_{4444}]$[D-Phe]-based SLBS achieve an *e.e.* of 51 ± 3% in a single step.

Author statement

Mariam Kholany: Investigation, Visualization, Writing - Original Draft

Francisca A. e Silva: Conceptualization, Methodology, Writing - Review & Editing

Tânia E. Sintra: Conceptualization, Methodology, Writing - Review & Editing, Funding acquisition

Paula Brandão: Methodology, Writing - Review & Editing

Sónia P. M. Ventura: Supervision, Writing - Review & Editing

João A. P. Coutinho: Conceptualization, Methodology, Supervision, Writing - Review & Editing, Funding acquisition